THE JOURNAL OF PHYSICAL CHEMISTRY B

ARTICLE

pubs.acs.org/JPCB

Exploring the Mechanism of Fluorescence Quenching in Proteins Induced by Tetracycline

Uttam Anand, Chandrima Jash, Ravi Kiran Boddepalli, Aseem Shrivastava, and Saptarshi Mukherjee*

Department of Chemical Sciences, Indian Institute of Science Education and Research, Bhopal ITI Campus (Gas Rahat) Building, Govindpura, Bhopal 462 023, Madhya Pradesh, India

ABSTRACT:

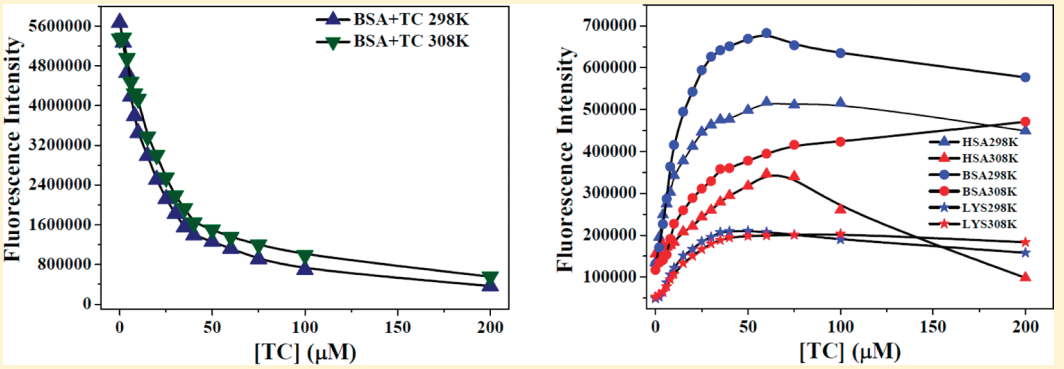

The binding of the antibiotic tetracycline hydrochloride (TC) to three proteins was investigated by steady-state, time-resolved, and circular dichroism spectroscopy. The tryptophan (Trp) amino acid residues were used as an intrinsic fluorophore to decipher the structure−function relationship. As monitored by CD spectroscopy, the addition of TC causes the protein to alter some of its helical content although such changes are only marginal. The gradual decrease in fluorescence intensity of Trp can be ascribed to static quenching which takes place by the interaction of the drug with the protein. Besides Trp quenching, there is evidence of fluorescence resonance energy transfer (FRET) in all three proteins with different values of efficiency of energy transfer. Various quenching/binding and thermodynamic parameters associated with such drug−protein interactions have been estimated. The results thus obtained can provide guidelines to synthetic chemists to design and synthesize target-oriented drugs.

INTRODUCTION

The binding of drugs to proteins has been recognized as an important factor in drug availability, drug efficacy, and drug transport for many years.[1] Although the topic of drug−protein interactions has drawn considerable research interest of late and has been extensively studied,[2−6] the mechanism of such interactions is still not clear. Among such drug−protein interactions, the use of tetracyclines (TC) occupies a seminal position.[7,8] TC molecules consist of four linearly fused tetracyclic nuclei (rings designated as A, B, C, and D, Scheme 1) to which a variety of functional groups are attached. TCs are a group of broad spectrum antibiotics which act as protein synthesis inhibitors, inhibiting the binding of aminoacyl-tRNA to the mRNA−ribosome complex, mainly by binding to the 30S ribosomal subunit in the mRNA complex.[9] Photosensitive and phototoxic properties[10] of TC causing skin lesions,[11] papular eruptions,[12] and formation of multinucleated giant cells[13] have been documented. These drugs after ingestion are solubilized inside the gut and are subsequently transported to the target sites through blood, bound to serum proteins.

Human serum albumin (HSA) is the most abundant protein in the circulatory system and is responsible for the binding and transport of a wide variety of fatty acids, drug molecules, and metabolites to their molecular targets.[14] It is a single polypeptide chain having 585 amino acid residues, characterized by low tryptophan and high cysteine content.[15] The secondary structure of the protein consists of 67% α-helix having 6 turns and 17 disulfide bridges.[16] Under physiological conditions, HSA adopts a heart-shaped three-dimensional structure having three homologous domains I−III.[15] Each of these three domains are further subdivided into two subdomains A and B that consist of 4 and 6 α-helices, respectively.[14,15] Using X-ray crystallography, He and Carter showed that the two halves of the albumin molecule form a 10 Å wide and 12 Å deep crevice that house a single tryptophan (W214) residue in the binding site IIA of the protein.[15] In spite of the complexity in shape and size, HSA has only a single tryptophan (Trp) residue, which makes it very convenient to study the structure and dynamics of the protein using intrinsic fluorescence.

Received: January 27, 2011
Revised: April 7, 2011
Published: April 27, 2011

Scheme 1. Structure of Tetracycline

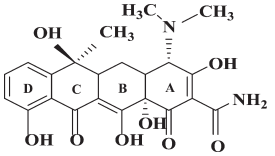

The globular protein bovine serum albumin (BSA) functions biologically as a carrier for fatty acid anions and other simple amphiphiles in the bloodstream, and it has 76% sequence homology with HSA. It is a single polypeptide chain having a molecular weight of ∼66 kDa and consists of 583 amino acid residues. There are 17 disulfide bridges and one free −SH group, which can cause it to form a covalently linked dimer. While both charged amino acid residues and apolar patches cover the interface, the interior of the protein is almost hydrophobic in nature.[14,17−19] BSA is characterized by three domains, each consisting of a large and a small double loop and a short and a long (hinge) connecting segment, whereas the next domain houses another large double loop and a connecting segment. The fundamental difference between HSA and BSA is that the former contains only one tryptophan amino acid residue (W214), while the latter has two, W212 and W135, out of which W135 seems to be rather dormant.[14]

Lysozyme (LYS) is a small monomeric low molecular weight (∼14 kDa) globular protein that contains α-helix, β-sheet turns and disordered structural elements. LYS is present in the mucosal secretion such as saliva and tears and is used as an agent to break into the host bacterial cells. It consists of 129 tactic amino acid residues containing six tryptophan and three tyrosine amino acid residues and four disulfide bonds.[20,21] The six tryptophan residues are located at the substrate binding sites, out of which two are in the hydrophobic matrix box, while one is separated from the others.[22] Among them, W62 and W108 are the most dominant fluorophores, both being located at the substrate binding site.[23] LYS has many physiological and pharmaceutical functions, such as antibacterial, antiviral, etc. Another important function of this protein is their ability to carry drugs to the target receptors, whereby the effectiveness of such drug targeting depends on their binding abilities.

Despite having complex structural features, these proteins have tryptophan amino acid residues which can be used as an intrinsic fluorophore and can investigate the effect of other substrates that bring about structural changes. In this present study, we have monitored the fluorescence emission of the proteins as a function of the added TC concentration, and fluorescence data clearly reveal that there is a quenching of fluorescence intensity with an increase of TC concentration. In all the three proteins studied here, the most interesting part is that, besides quenching, there is a decrement in tryptophan emission owing to fluorescence resonance energy transfer (FRET) which is clear from the emission spectra, whereby there is a slight rise in emission intensity characteristic of TC. Time-resolved measurements also support the fact that there is a gradual decrease in the lifetime of tryptophan with the increase of TC concentration. Steady-state experiments were done at two different temperatures (298 and 308 K), and using Stern−Volmer and modified Stern−Volmer equations, we have estimated various binding and thermodynamic parameters. These results suggest that binding decreases with the rise of temperature. Beyond a fixed concentration of TC, there is a structural deformation of the proteins, and this fact is also well supported by circular dichroism (CD) data.

In the present work, we have investigated the effect of the drug tetracycline hydrochloride (TC, Scheme 1) on three globular proteins, namely human serum albumin (HSA), bovine serum albumin (BSA), and lysozyme (LYS). We have studied the structural changes of the proteins brought in by TC using CD spectroscopy and have used steady-state (absorption and emission) and time-resolved measurements to characterize the effect of the added TC to the protein. Stern−Volmer and modified Stern−Volmer plots have been used to study the mechanism of quenching of the intrinsic fluorescence of tryptophan in the protein moieties initiated by the added drug molecules. FRET between Trp (donor) and TC (acceptor) has been investigated, and the distance between the donor and acceptor has been estimated for all the three proteins.

EXPERIMENTAL SECTION

a. Materials. Human serum albumin (HSA) and bovine serum albumin (BSA) were purchased from Sigma, essentially fatty acid free and globulin free. Lysozyme (LYS), from chicken egg white, was purchased from Fluka. Tetracycline hydrochloride (TC, molecular weight = 480.9) was purchased from HIMEDIA and was used as received. All solutions were prepared in 50 mM Tris buffer, pH = 7.5. For steady-state fluorescence measurements, the temperature was controlled using a Thermo Electron Corporation chiller. Temperature during all other experiments was maintained at 25 °C ± 0.1 °C, unless otherwise mentioned.

b. Steady-State Measurements. Steady-state absorption measurements were carried out in a Perkin-Elmer UV−vis spectrophotometer, Lambda-25. All the steady-state fluorescence measurements were recorded on a HORIBA Jobin Yvon, Fluorolog 3−111. A 10 μM protein solution was used to record the spectra in a 50 mM Tris buffer solution having a pH = 7.5 with varying concentrations of TC. The fluorescence spectra were measured with a 10 mm path length quartz cuvette. HSA, BSA, and LYS were excited at 295 nm in order to minimize the contribution from tyrosine. The fluorescence emission was collected from 305 to 580 nm with an integration time of 0.1 s. The emission and the excitation slits were kept at 5 and 1.5 nm, respectively.

c. Time-Resolved Fluorescence Measurements. For lifetime measurements, the samples were excited at 295 nm using a picosecond diode (IBH-NanoLED source N-295). The emission was collected at magic angle polarization using a Hamamatsu MCP photomultiplier (model R-3809U-50). The time-correlated single photon counting (TCSPC) setup consists of an Ortec 9327 pico-timing amplifier. The data was collected with a PCI-6602 interface card as a multichannel analyzer. The typical full width at half maximum (fwhm) of the system response was about 800 ps.

d. Circular Dichroism Spectroscopy Measurements. Circular dichroism (CD) measurements were carried out on an Applied Photophysics (U.K.) (model CIRASCAN) spectropolarimeter equipped with a Peltier temperature controller. All the CD measurements were performed at 298 and 308 K with an accuracy of ±0.1 K. Spectra were collected with a scan speed of 200 nm/min with a spectral bandwidth of 10 nm. Each spectrum was the average of four scans. Secondary structure (far-UV CD)

was measured over the wavelength range of 200−250 nm using a 0.1 cm path length cuvette. Buffer solutions containing the corresponding concentration of TC were subtracted from all the measurements. The results were expressed as mean residue ellipticity (MRE) in deg cm^2 dmol^{-1} which is defined as

$$\mathrm{MRE} = \frac{\theta_{\mathrm{obs}}(m\mathrm{deg})M}{nlC} \quad (1)$$

where θ_{obs} is the CD in millidegrees, M is the molecular weight of the protein in g dmol^{-1}, n is the number of amino acid residues (585, 583, and 129 in the case of HSA, BSA and LYS, respectively), l is the path length (0.1 cm) of the cuvette, and C is the concentration of the protein in g L^{-1}.

RESULTS AND DISCUSSIONS

a. Circular Dichroism Spectroscopy. Circular dichroism (CD) spectroscopy is vastly used in monitoring the structure, conformation, and stability of proteins in solutions.[24−27] CD probes the secondary structure of proteins because the peptide bond is asymmetric and molecules without a plane of symmetry show the phenomena of CD. Although CD cannot provide the details regarding the precise structure of proteins, nevertheless it can provide us with a very good estimation of the fraction of the residues in the protein structure which are involved in α-helix, β-sheet, and disorderly formation (random coil). In order to decipher the structural and conformational changes brought in by the added TC molecules, we have performed CD spectral studies of the three different proteins (HSA, BSA, and LYS) in the presence of varying concentrations of TC. Figure 1 shows the representative CD spectra of BSA both in the absence and presence of TC of varying molar ratios. It is evident from the figure that the CD spectra for BSA (and also HSA, figure not shown) show two minima at 208 and 222 nm, which is a clear signature of the presence of α-helix in the protein under study. The CD spectra of LYS is rather complicated, and it has significant contributions from α-helix, β-sheet, and disorderly formation (random coil). In their native forms, the percentage α-helix of HSA, BSA, and LYS has been estimated to be 65%, 60%, and 35%, respectively, and our data suggests almost similar values.[28] It was interesting to observe that addition of TC to both HSA and BSA in small molar ratios, up to 1:1 (TC:BSA or HSA), actually causes marginal destabilization of the protein α-helical content. For HSA and BSA, the percentage of α-helix corresponding to a molar ratio of 1:1 has been estimated to be about 64% and 57%, respectively. Thus, the added TC brings in some destabilization to the proteins (HSA and BSA) as mentioned earlier. Beyond a molar ratio of 1:1, the CD spectra exhibit a signature of the protein (both HSA and BSA) getting stabilized, and the α-helix for HSA and BSA increases to about 66.5% and 65% (for a molar ratio 2:1) and to about 65% and 64.5%, respectively (for a molar ratio 4:1). These features are evident from Figure 1 and Table 1. Similar results have also been observed by Khan and co-workers[29] who opined that the increase in the magnitude of MRE at 222 and 208 nm was indicative of stabilization of helical structure of the two forms (N and B) of HSA beyond a drug:HSA molar ratio of more than 1.0. However, in the case of LYS, the MRE values are indicative of the fact that the added TC molecules start to stabilize the protein even at low molar ratios of TC:LYS (Table 1), and the α-helix increases to about 39% at a molar ratio of 1:1. On the basis of our observations, we can conclude that the added TC does not bring about major structural deformations of the proteins.

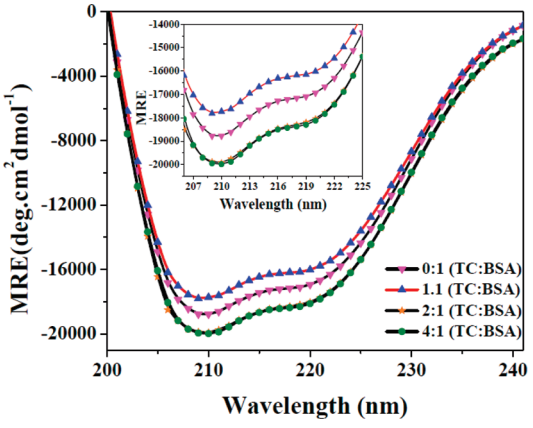

Figure 1. Circular dichroism (CD) spectra of BSA under different molar ratios of TC:BSA as marked in the figure. The inset represents the zoomed in version having better clarity.

Although the knowledge of CD spectroscopy gives us an estimate of the overall global structural changes induced by the added drug molecule, it cannot furnish us with the requisite information regarding the local environment in and around the tryptophan or the binding sites of TC. For the above said purpose, we investigated the systems using spectroscopic techniques which are supposedly more precise and accurate in deciphering the microenvironmental changes brought in by the added TC molecules.

b. Tetracycline Induced Fluorescence Quenching of Proteins. On increasing the concentration of TC in the protein solutions under investigation, the absorbance or optical density (O.D.) values increases almost monotonically. For fluorescence experiments, the O.D. corrected values were used in order to avoid the inner filter effect. For fluorescence studies, the tryptophan amino acid residues of the proteins were used as an intrinsic fluorophore, and the samples were excited at 295 nm in order to

Table 1. MRE Values at 208 and 222 nm under Different Ratios of TC:Protein at 298 K

	HSA		BSA		LYS	
TC:protein	MRE_{222} (deg cm^2 dmol^{-1})	MRE_{208} (deg cm^2 dmol^{-1})	MRE_{222} (deg cm^2 dmol^{-1})	MRE_{208} (deg cm^2 dmol^{-1})	MRE_{222} (deg cm^2 dmol^{-1})	MRE_{208} (deg cm^2 dmol^{-1})
0:1	−19 939	−15 300	−17 152	−12 577	−6241	−8220
1:1	−19 626	−15 115	−16 178	−12 015	−7284	−8984
2:1	−20 237	−15 738	−18 289	−13 939	−8563	−10 599
4:1	−20 077	−15 373	−18 370	−13 671	−6871	−8838

dx.doi.org/10.1021/jp2008978 |J. Phys. Chem. B 2011, 115, 6312–6320

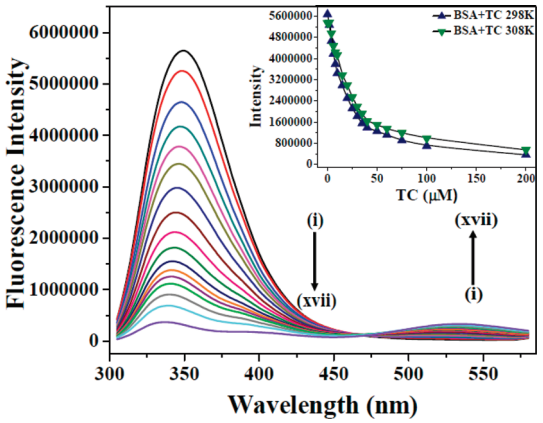

Figure 2. Fluorescence spectra of 10 μM BSA in the absence and presence of various concentrations of TC: (i) BSA in the absence of TC; (ii−xvii) emission spectra of BSA in the presence of 2, 4, 6, 8, 10, 15, 20, 25, 30, 35, 40, 50, 60, 75, 100, and 200 μM TC, respectively. The samples were excited at 295 nm to minimize the contribution of tyrosine. The inset represents the fall of Trp fluorescence intensity with increasing concentration of TC.

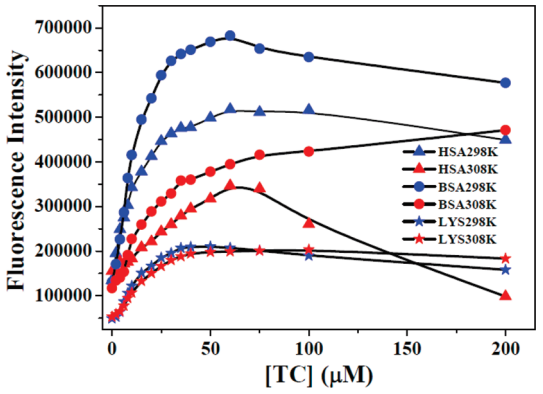

Figure 3. Plot of fluorescence intensity of TC against the varying concentrations of TC to have an estimate of the saturating concentration of TC binding at 298 and 308 K. The samples were excited at 365 nm.

minimize the contribution of tyrosine. In order to investigate the effect of temperature on the binding of TC to the proteins, we have carried out emission studies at two different temperatures, 298 K (25 °C) and 308 K (35 °C). At 298 K, the emission maxima of HSA, BSA, and LYS alone in buffer were recorded to be centered at 347, 350, and 345 nm, respectively. Figure 2 shows the representative fluorescence spectra of BSA at 298 K, both in the absence and presence of varying concentrations of TC. Even at 308 K, the emission peaks of Trp do not show any appreciable deviation from those recorded at 298 K. When TC is added to a solution containing 10 μM protein, the added drug molecule gets attached to a site very close to that of the Trp amino acid residue, i.e., in site I of domain IIA in case of HSA and BSA[30] and in the hydrophobic box of LYS containing W108 and W62.[31] The inset of Figure 2 represents the nonlinear fall of emission intensity of Trp with the increasing concentration of TC for BSA at 298 and 308 K. For HSA and LYS, similar trends are followed at both temperatures (figures not shown). Besides exhibiting a fluorescence quenching, the emission maxima of Trp for all the three proteins display a blue shift at both temperatures. At 298 K, the emission maximum of Trp is blue-shifted by 7, 10, and 11 nm for

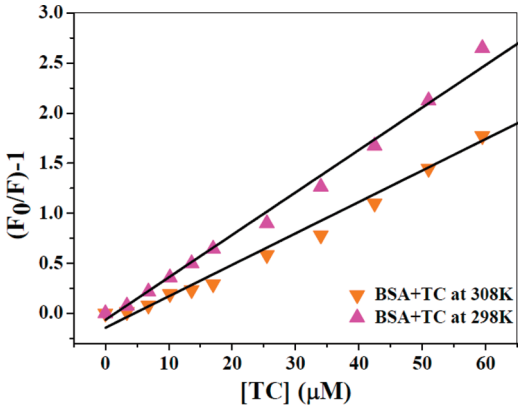

Figure 4. Stern−Volmer plots for BSA against varying concentrations of TC at 298 and 308 K.

HSA, BSA, and LYS, respectively, when the TC concentration is 60 μM. Almost similar blue-shifted spectra are recorded at 308 K. This blue shift in emission wavelength is due to increase in hydrophobicity in and around Trp with increase in TC concentration. It is worth mentioning here that the steady-state fluorescence spectra monitor the local microenvironment in and around the Trp amino acid residue, unlike what is encountered in our CD data where the global picture is elucidated.

For monitoring the TC fluorescence in the presence of proteins, the solutions were also excited at 365 nm (which happens to be the absorption maximum of TC), and it was observed that, for all the three proteins, the fluorescence intensity of TC first increases up to 60 μM and then either saturates or shows a decrease (Figure 3). From Figure 3, it is evident that, with a protein concentration of 10 μM, the binding of TC saturates at around 60 μM, beyond which the phenomenon of self-quenching may be operational. The added TC molecules do bring about quenching of the Trp fluorescence of the proteins, but the fluorescence of TC (when excited at 365 nm) does not have any appreciable effect on the fluorescence of the proteins under investigation.

In order to understand drug−protein interaction, the concept of fluorescence quenching has been widely used.[32−35] Fluorescence quenching is operational mainly by two mechanisms, static (by complex formation) and dynamic (collisional processes). In the case of the former, with rise in temperature, the stability of the formative compound will be reduced, and thereby, the quenching constant will also be lowered. On the other hand, in dynamic quenching (which happens to be diffusion driven), the effective number of colliding ions increases, enhancing the transfer of energy and thereby increasing the quenching constant of the fluorescent substance with the rise of temperature. The fluorescence quenching data of Trp were analyzed according to the Stern−Volmer equation:[36]

$$\frac{F_0}{F} = 1 + k_q \tau q_0 [Q] = 1 + K_{SV}[Q] \qquad (2)$$

In the above equation, F_0 and F are the fluorescence peak intensities of the fluorophore (Trp) in the absence and presence of quencher. [Q] is the quencher (TC in the present case) concentration, and K_{SV} is the Stern−Volmer quenching constant. k_q is the bimolecular quenching constant, and τ_0 is the average lifetime of the protein without quencher. The value of τ_0 is generally taken to be 10^{-8} s.[36] Figure 4 represents the

Table 2. Quenching Constants and Binding Parameters of Protein + TC Systems at 298 and 308 K

	HSA (298 K)	HSA (308 K)	BSA (298 K)	BSA (308 K)	LYS (298 K)	LYS (308 K)
K_{SV} (L mol^{-1})	5.38×10^4	3.64×10^4	7.21×10^4	5.33×10^4	7.40×10^4	5.21×10^4
K_A (L mol^{-1})	9.49×10^4	4.20×10^4	9.03×10^4	5.22×10^4	7.98×10^4	5.56×10^4
K_a (L mol^{-1})	7.80×10^4	2.15×10^4	4.47×10^4	1.91×10^4	4.04×10^4	2.33×10^4
n	0.57	1.01	1.00	1.43	1.02	1.17

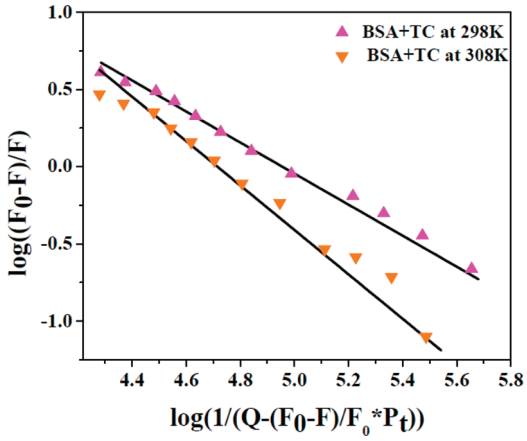

Figure 5. Plot of $\log[(F_0 - F)/F]$ against $\log(1/[Q_t] - \{(F_0 - F)[P_t]\}/F_0)$ at 298 and 308 K for BSA and various concentrations of TC. This plot gives us an estimate regarding the binding parameters.

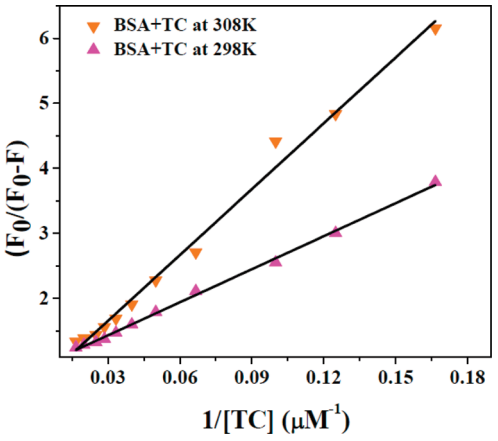

Figure 6. Plot of $(F_0/F_0 - F)$ against $1/[Q]$ for BSA at 298 and 308 K as per the modified Stern–Volmer equation.

Stern–Volmer plots of BSA in the presence of various concentrations of TC at two different temperatures. Since the binding of TC to the proteins gets almost saturated at 60 μM (please refer Figure 3), we have fit the graphs up to that concentration of TC. For the other two proteins, HSA and LYS, similar graphs have been obtained (figures not shown), and the K_{SV} values of all the proteins have been summarized in Table 2. From Figure 4, it is evident that the graphs at both the temperatures show an upward trend indicating that both static and dynamic quenching is operational when TC is added to the protein. From the nature of the Stern–Volmer graphs as depicted in Figure 4 and as seen from Table 2, the magnitudes of K_{SV} decrease with rise of temperature, which is a sufficient indication of static quenching, which is the principle reason of fluorescence quenching of Trp, although dynamic quenching is also operative which adds on to the fluorescence decrement. Besides estimating the magnitude of Stern–Volmer constants using eq 2, we can further estimate the apparent binding constant (K_A) and the binding affinity (n) by plotting $\log[(F_0 - F)/F]$ against $\log(1/[Q_t] - \{(F_0 - F)[P_t]\}/F_0)$ by using the following equation.[37,38]

$$\log[(F_0 - F)/F] = n \log K_A - n \log(1/[Q_t] - \{(F_0 - F)[P_t]\}/F_0) \quad (3)$$

Here, $[Q_t]$ and $[P_t]$ are the total quencher concentration and total protein concentration, respectively. Using the fluorescence intensity values of Trp under various concentrations of TC at both the temperatures, we have estimated the values of K_A and n, and the parameters are summarized in Table 2. Figure 5 represents a plot of $\log[(F_0 - F)/F]$ against $\log(1/[Q_t] - \{(F_0 - F)[P_t]\}/F_0)$ for BSA under various concentrations of TC at both the temperatures. For HSA and LYS, similar plots are obtained, and the corresponding K_A and n values are estimated (Table 2).

From the values of K_A at the two different temperatures, it is evident that its magnitude decreases with the rise of temperature. The affected quenching constant (K_a) has been estimated using the following modified Stern–Volmer equation:[33]

$$\frac{F_0}{F_0 - F} = \frac{1}{f} + \frac{1}{K_a f} \times \frac{1}{[Q]} \quad (4)$$

Here, f is the fraction of the accessible fluorophore. Figure 6 represents a plot of $(F_0/F_0 - F)$ against $1/[Q]$ for BSA at both the temperatures, and from the slopes of the curves, the values of K_a have been estimated and summarized in Table 2. Similar linear curves were also obtained for HSA and LYS. From Table 2, it can be seen that the values of K_a decrease with the rise in temperature which agrees with the temperature dependence of K_{SV}. All these values are indicative of the phenomenon of static quenching which is the driving force for the fall in Trp emission with the rise of TC concentrations.

Estimation of Thermodynamic Parameters. Thermodynamic parameters, such as free energy of binding ($\Delta G^\circ_{Binding}$), enthalpy (ΔH°), and entropy (ΔS°), play a pivotal role in controlling the interactions associated with drug–protein interactions, and hence they need to be reviewed. In order to have an estimate of the three thermodynamic parameters mentioned above, we used the following equations:

$$\Delta G^\circ_{Binding} = -2.303RT \log K = \Delta H^\circ - T\Delta S^\circ \quad (5)$$

$$\ln K_2/K_1 = (1/T_1 - 1/T_2)\Delta H^\circ/R \quad (6)$$

K_1 and K_2 are the apparent binding constants (K_A) at temperature T_1 (298 K) and temperature T_2 (308 K), respectively and R is the universal gas constant. Table 3 summarizes the thermodynamic parameters for all three proteins at the two temperatures under consideration. As per the discussions by Ross and

dx.doi.org/10.1021/jp2008978 |J. Phys. Chem. B 2011, 115, 6312–6320

Table 3. Thermodynamic Parameters of Protein + TC Systems at 298 and 308 K

	HSA (298 K)	HSA (308 K)	BSA (298 K)	BSA (308 K)	LYS (298 K)	LYS (308 K)
$\Delta G°$ (J mol^{-1})	-2.84×10^4	-2.73×10^4	-2.83×10^4	-2.78×10^4	-2.79×10^4	-2.79×10^4
$\Delta H°$ (J mol^{-1})	-6.22×10^4	-6.22×10^4	-4.18×10^4	-4.18×10^4	-2.77×10^4	-2.77×10^4
$\Delta S°$ (J K^{-1} mol^{-1})	−113.2	−113.3	−45.55	−45.55	1.05	1.05

Subramanian,[39] the negative $\Delta H°$ and $\Delta S°$ values are associated with hydrogen bonding and van der Waals interaction in low dielectric medium. Very low positive and negative values of $\Delta H°$ and positive $\Delta S°$ values are characteristic of electrostatic interactions.[39] Whenever a drug (or ligand) binds to a protein, then the associated water (or solvent) molecules are displaced due to such interactions or binding. This large number of solvent molecules is responsible for a positive entropy change of the entire system as a whole during the initial attachment of the drug to the protein.[39] Subsequently, forces such as hydrogen bonding, van der Waals, and electrostatic interactions become predominant and control the overall thermodynamic parameters. In our present systems, the proteins bear net overall charges and the drug (TC) is ionizable in nature. As seen from Table 3, the magnitudes of $\Delta G°_{binding}$ are all negative at both the temperatures, signifying that the processes of drug−protein interactions are all spontaneous in nature. What is more interesting is that the magnitudes of $\Delta H°$ out-weigh those of $\Delta S°$, thereby exemplifying the fact that the interactions are rather enthalpy and not entropy driven. Once the drug has been incorporated inside the protein, there is a competition between electrostatic and hydrophobic interactions. As mentioned earlier, positive $\Delta S°$ values are indicative of electrostatic interactions; from the sign of $\Delta S°$ we can conclude that, for both BSA and HSA, it is the hydrophobic interactions that are predominant over the electrostatic ones, thereby making the final value of $\Delta S°$ negative. For LYS, the very small magnitude of $\Delta S°$ suggests that here both electrostatic and hydrophobic interactions are almost equally predominant, hence the small positive value. Nevertheless, for all three proteins under consideration, enthalpy plays a major role, as discussed above.

Steady-State FRET. The nonradiative fluorescence resonance energy transfer occurs between a FRET pair, whereby the primary requirement is that there should be a spectral overlap between the emission of the donor (Trp in the present study) and the absorption of the acceptor (TC in the present case). According to the Förster nonradiation energy transfer theory,[36] the energy transfer efficiency (E) is related not only to the distance (r_0) between acceptor and donor, but also to the critical energy transfer distance (R_0), i.e.

$$E = \frac{R_0^6}{R_0^6 + r_0^6} \tag{7}$$

where R_0 is a characteristic distance, called the Förster distance or critical distance at which the energy transfer efficiency is 50%. The magnitude of R_0 can be estimated using the following equation[36]

$$R_0^6 = 8.8 \times 10^{-25} \kappa^2 N^{-4} \phi J \tag{8}$$

where κ^2 is the spatial orientation factor describing the relative orientation in space of the transition dipoles of the donor and acceptor, N is the refractive index of the medium, ϕ is the fluorescence quantum yield of the donor in the absence of acceptor, and J is the overlap integral between the donor fluorescence emission spectrum and the acceptor absorption spectrum. The magnitude of J is given by

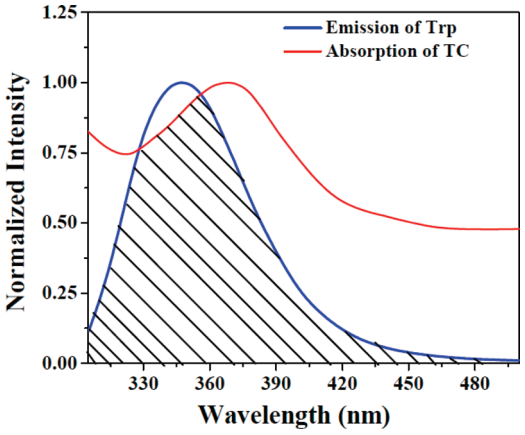

Figure 7. Normalized overlap emission spectrum of BSA (blue) with that of the absorption spectrum (red) of TC. The shaded region resembles the actual overlap of both the spectra.

$$J = \frac{\sum F(\lambda)\varepsilon(\lambda)\lambda^4 \Delta\lambda}{\sum F(\lambda)\Delta\lambda} \tag{9}$$

where $F(\lambda)$ is the fluorescence intensity of the donor at wavelength λ, and $\varepsilon(\lambda)$ is the molar absorption coefficient of the acceptor at that wavelength (λ) expressed in M^{-1} cm^{-1}. E can also be estimated using the fluorescence emission intensity both in the absence and presence of acceptor by using the following equation:

$$E = 1 - \frac{F}{F_0} \tag{10}$$

In Figure 7, we have plotted the overlap of the emission spectra of BSA with that of the absorption spectra of TC. The figure is a clear signature of the FRET process that is operational in the presence of the quencher, TC. J values for all three protein−TC systems have been calculated by integrating the overlap spectra (figure not shown for HSA and LYS) from 305 to 500 nm wavelength region and were found to be 2.74×10^{-15}, 2.68×10^{-15}, and 2.78×10^{-15} for HSA, BSA, and LYS, respectively. Putting the values of $\kappa^2 = {}^2/_3$, $N = 1.45$, and $\phi = 0.118$, and using eqs 7−10, the distance (r_0) between the drug (TC) and Trp amino acid residue for the three proteins has been summarized in Table 4. From the table it is evident that the value of r_0 (as obtained from steady-state FRET) is pretty close to that of R_0, the Förster distance or critical distance at which the energy transfer efficiency is 50%. It must be mentioned here that when we are monitoring FRET by steady-state measurements, we are actually overestimating the values of r_0 as the steady-state measurements have the contribution from static quenching which seems to be the principal reason for the lowering of the donor fluorescence emission. Hence, to have a better understanding of

Table 4. Steady-State and Time-Resolved FRET Parameters

system	R_0 (nm)	$\langle E_{FRET}\rangle$ (from steady-state)	r_0 (nm) (from steady-state)	$\langle E_{FRET}\rangle$ (from time-resolved)	r_0 (nm) (from time-resolved)
HSA + TC	1.871	48.20	1.893	2.955	3.347
BSA + TC	1.876	47.40	1.908	2.490	3.456
LYS + TC	1.864	45.00	1.928	4.655	3.084

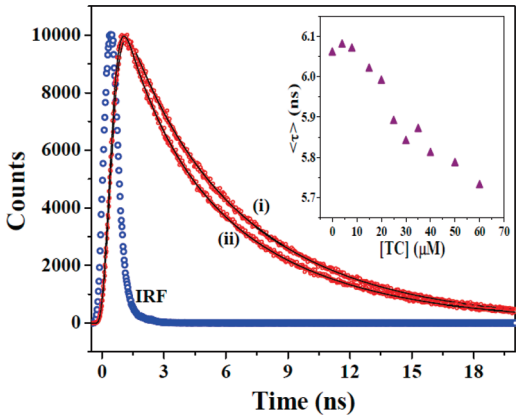

Figure 8. Fluorescence lifetime decays of BSA (i) in the absence of TC and (ii) in the presence of 60 μM TC. The scattered points represent the actual decay profile while the solid blue line represents a biexponential fit to that decay. The inset represents the fall of the average lifetime ($\langle\tau\rangle$) with increasing concentration of TC.

the exclusive FRET present in the system, we need to characterize the systems using time-resolved measurements.

c. Time-Resolved Fluorescence Quenching of Proteins in the Presence of Tetracycline. The investigation of intrinsic fluorescence from proteins has been regarded as an effective method to study protein conformational dynamics. Protein fluorescence can be complex as well as very challenging to explain but has been a topic of interest of late. In spite of the fact that the structures of HSA, BSA, and LYS are rather complicated, they have been widely studied by making use of the Trp residue which is used as an intrinsic fluorophore. In aqueous solutions at neutral pH, Trp exhibits multiple exponential decays, and this has been attributed to the existence of rotational conformational isomers, called rotamers.[36,40] These rotamers play a significant role in determining the lifetimes of Trp in organized media: during the process of quenching, there are interactions of the quencher molecules with that of the substrate. This leads to the distortion of the indole ring planarity thereby changing the local environment around the Trp causing a decrement in the lifetime.[40] In our present work, we have investigated the effect of various concentrations of TC on the lifetimes of the three proteins. Figure 8 shows representative decays of BSA in buffer and in the presence of 60 μM TC. From the decay curves it is readily seen that the reduction of lifetime even in the presence of saturating condition of TC (60 μM) is only marginal. Similar decay profiles are also obtained for HSA and LYS (figures not shown), and the decay parameters for all the three proteins are summarized in Table 5.

As mentioned earlier, the principal reason for the quenching of Trp fluorescence is the static quenching induced by the added TC. However, a contribution from dynamic quenching cannot be ruled out which is also pertinent in the emission intensity curve (please refer Figure 2) where a small magnitude of FRET is

Table 5. Fluorescence Lifetimes of Proteins as a Function of Concentrations of TC

system	a_1	τ_1 (ns)	a_2	τ_2 (ns)	$\langle\tau\rangle^a$ (ns)	χ^{2b}
HSA (10 μM)						
+TC (0 μM)	21.11	2.64	78.89	6.68	5.82	1.08
+TC (15 μM)	17.69	2.20	82.31	6.39	5.64	1.24
+TC (40 μM)	21.89	2.41	78.11	6.47	5.58	1.02
+TC (60 μM)	24.93	2.60	75.07	6.55	5.56	1.10
BSA (10 μM)						
+TC (0 μM)	11.39	2.83	88.61	6.48	6.06	1.14
+TC (15 μM)	16.72	2.98	83.28	6.63	6.02	1.06
+TC (40 μM)	13.00	2.24	87.00	6.34	5.81	1.02
+TC (60 μM)	14.43	2.15	85.57	6.33	5.73	1.08
LYS (10 μM)						
+TC (0 μM)	62.98	1.42	37.02	3.08	2.04	1.06
+TC (15 μM)	55.08	1.27	44.92	2.83	1.97	1.09
+TC (40 μM)	52.85	1.21	47.15	2.68	1.90	1.12
+TC (60 μM)	52.83	1.14	47.17	2.67	1.86	1.02

[a] $\langle\tau\rangle = a_1\tau_1 + a_2\tau_2$. [b] The magnitude of χ^2 denotes the goodness of the fit.

exemplified. From Table 4, it can be seen that the time-resolved energy transfer efficiency (E) is much lower than those estimated from steady-state measurements. The magnitudes of E_{FRET} in columns 3 and 5 of Table 4 represent those estimated from steady-state and lifetime measurements, respectively. As stated earlier, the magnitude of E_{FRET} as obtained from steady-state data is overestimated, and since static quenching (which is estimated from steady-state measurements) is the principal reason for fluorescence decrement of Trp, the values of E_{FRET} in column 3 of Table 4 are higher than those mentioned in column 5. As evidenced from Figure 2, the mechanism of FRET is indeed operational, but the small increment of fluorescence intensity of the acceptor (TC in the present case) reflects the small magnitude of E_{FRET} as seen in column 5 of Table 4. The magnitudes of E_{FRET} in column 5 are obtained from lifetime measurements, and since there is a marginal decrement of lifetime upon the addition of TC, there is a loss in magnitude of E_{FRET} in column 5 as compared to column 3 of Table 4. The decrease in lifetime occurs because quenching is an additional rate process that depopulates the excited state.[36] The decrease in yield occurs because quenching depopulates the excited state without fluorescence emission. It is interesting to note that static quenching does not decrease the fluorescence lifetime because only those fluorescence molecules which do not form complexes contribute toward decreasing the lifetime. These uncomplexed fluorophore molecules (which suffer collisional quenching) thus have almost exclusive contribution toward dynamic quenching.[36] Thus, the values of E obtained from lifetime measurements exclusively report the process of dynamic quenching, and the emission peak at around 530 nm is supportive of the process of

FRET that is present in the presence of TC. The magnitude of E is obtained using the following equation

$$E = 1 - \frac{\tau}{\tau_0} \quad (11)$$

where τ and τ_0 are the lifetimes of Trp in the presence and absence of TC, respectively. Upon binding with TC, the nonradiative pathways in Trp, mainly the charge transfer process from the indole ring to a nearby substituent, are enhanced, and therefore there is a marginal shortening of lifetime. Besides this, the effect of dielectric constant in altering the lifetime of the system needs to be considered. Depending on the solvent's properties and the extent of ion association/dissociation, the values of dielectric constants for the electrolyte solution may increase or decrease with rising electrolyte concentration.[41] For example, addition of alkali and alkaline earth halides to water and methanol results in a decrease in the dielectric constant of the solution. On the other hand, solutions of onium salts (e.g., Bu_4NBr, Bu_4NClO_4, and i-Pen_4NNO_3) in solvents of low and medium permittivity have dielectric constants that increase with the salt concentration.[41] In the present case, the added TC molecules, which contain four linearly fused tetracyclic nuclei, may actually marginally increase the dielectric constant by adsorption to the protein surface. However, the concentrations of TC are pretty low (in micromolar concentrations), and hence the added TC will most likely have no contribution in altering the dielectric constant of the medium. Therefore, this should not have any effect on the magnitudes of fluorescence lifetime. As seen from Table 5, the amplitudes of the respective slow and fast components of lifetime (a_1 and a_2) also do not exhibit appreciable changes upon the addition of TC, proving that since there is no major structural change induced, the interconversion of the various rotamers of Trp is hindered. The estimated distances between the donor (Trp) and acceptor (TC) for all three proteins are almost similar and lie between the Förster's distance range (2−8 nm) which corroborates the fact that FRET is indeed operational when the fluorescence emission of Trp is getting quenched by the subsequent additions of TC. So by using time-resolved measurements, we have exclusively monitored the process of dynamic quenching and its contribution toward the overall decrement of fluorescence intensity of Trp which is otherwise missed during our steady-state measurements.

CONCLUSIONS

In the present work we have shown that the addition of the antibiotic TC causes the intrinsic fluorescence of Trp to get quenched. The actual mechanism of such quenching is static in nature which happens by the addition of the TC to the protein under investigation. We have studied three different proteins, and CD spectra for all three revealed that, even at saturating conditions of TC, the proteins change their helicity only by a small percentage. Steady-state and time-resolved spectroscopies were employed to characterize these systems under various concentrations of TC, and we have proven that although static quenching is the principle reason for the loss of Trp emission, dynamic quenching is also present which is monitored exclusively by the time-resolved measurements. The average lifetimes of Trp for all the three proteins change only marginally. The thermodynamic parameters as estimated from the Stern−Volmer and modified Stern−Volmer plots suggest that the binding of TC to the proteins is rather enthalpy and not entropy driven. The negative values of Gibbs' free energy are indicative of the fact that such additions are also spontaneous in nature.

AUTHOR INFORMATION

Corresponding Author

*E-mail: saptarshi@iiserbhopal.ac.in.

ACKNOWLEDGMENT

We sincerely thank Professor Vinod Kumar Singh, Director IISER Bhopal, for his constant encouragement and support. We also thank the Advanced Instrumentation Research Facility, Jawaharlal Nehru University (JNU), New Delhi, for helping us to carry out the CD spectroscopy experiment. S.M. thanks Dr. Lisha Kurup, Department of Chemical Sciences, IISER Bhopal, for providing us with the TC. S.M. also thanks Professor Anindya Datta, IIT Bombay, for many stimulating discussions. U.A. thanks IISER Bhopal for providing fellowship, and C.J. thanks DST for providing INSPIRE fellowship.

REFERENCES

(1) Watanabe, Y.; Hayashi, T.; Kitayama, R.; Yasuda, T.; Saikawa, I.; Shimizu, K. *J. Antibiot. (Tokyo)* **1981**, *34*, 753–757.
(2) Chen, J.; Hage, D. S. *Nat. Biotechnol.* **2004**, *22*, 1445–1448.
(3) Talbert, A. M.; Tranter, G. E.; Holmes, E.; Francis, P. L. *Anal. Chem.* **2002**, *74*, 446–452.
(4) Kratochwil, N. A.; Huber, W.; Müller, F.; Kansy, M.; Gerber, P. R. *Biochem. Pharmacol.* **2002**, *64*, 1355–1374.
(5) Koeplinger, K. A.; Zhao, Z. *Anal. Biochem.* **1996**, *243*, 66–73.
(6) Luo, R.-S.; Liu, M.-L.; Mao, X.-A. *Spectrochim. Acta, Part A* **1999**, *55*, 1897–1901.
(7) Chopra, I.; Roberts, M. *Microbiol. Mol. Biol. Rev.* **2001**, *65*, 232–260.
(8) Chopra, I. *Antimicrob. Agents Chemother.* **1994**, *38*, 637–640.
(9) Lehninger, , A.; Nelson, , D. L.; Cox, , M. M. *Lehninger's Principles of Biochemistry,* 5th ed.; Freeman Publishers: New York, 2008.
(10) Epstein, J. H.; Tuffanelli, D. L.; Seibert, J. S.; Epstein, W. L. *Arch. Dermatol.* **1976**, *112*, 661–666.
(11) Cullen, S. I.; Catalano, P. M.; Helfman, R. J. *Arch. Dermatol.* **1966**, *93*, 77.
(12) Frost, P.; Weinstein, G. D.; Gomez, E. C. *J. Am. Med. Assoc.* **1971**, *216*, 326–329.
(13) Zuehlke, R. L. *Arch. Dermatol.* **1973**, *108*, 837–838.
(14) Peters, T. *All About Albumin: Biochemistry, Genetics, and Medical Applications*; Academic: San Diego, 1996.
(15) He, X. M.; Carter, D. C. *Nature* **1992**, *358*, 209–215.
(16) Narazaki, R.; Maruyama, T.; Otagiri, M. *Biochim. Biophys. Acta* **1997**, *1338*, 275–281.
(17) Foster, J. F. In *Albumin Structure, Function and Uses*; Rosenoer, V. M., Oratz, M., Rothschild, M. A., Eds.; Pergamon Press Inc.: Oxford, U.K., 1977.
(18) Vijai, K.; Forster, J. *Biochemistry* **1967**, *6*, 1152–1159.
(19) Curry, S.; Mandelkow, H.; Brickm, P.; Franks, N. *Nat. Struct. Biol.* **1998**, *5*, 827–835.
(20) Gu, Z.; Zhu, X.; Ni, S.; Su, Z.; Zhou, H. M. *Int. J. Biochem. Cell Biol.* **2004**, *36*, 795–805.
(21) Fang, Y.; Yi, L.; Fang, Y. *Acta Chim. Sin.* **2003**, *61*, 803–807.
(22) Sheng, C. J.; Dian, H. D. *Lysozyme*; Shamdong Science and Technology Press, 1982; p 50.
(23) Imoto, T.; Foster, L. S.; Ruoley, J. A.; Tanaka, F. *Proc. Natl. Acad. Sci. U.S.A.* **1972**, *69*, 1151–1155.
(24) Corrêa, D. H. A.; Ramos, C. H. I. *Afr. J. Biochem. Res.* **2009**, *3*, 164–173.
(25) Parker, W.; Song, P.-S. *Biophys. J.* **1992**, *61*, 1435–1439.

(26) Johnson, W. C., Jr. *Annu. Rev. Biophys. Biophys. Chem.* **1988**, *17*, 145–166.
(27) Woody, R. W. Theory of Circular Dichroism of Proteins. In *Circular Dichroism and Conformational Analysis of Biomolecules*; Fasman, G. D., Ed.; Plenum Press Publisher: New York, 1996; p 25.
(28) Software downloaded free from the internet (www.embl.de/~andrade/k2d/).
(29) Ahmad, B.; Parveen, S.; Khan, R. H. *Biomacromolecules* **2006**, *7*, 1350–1356.
(30) Khan, M. A.; Muzammil, S.; Musarrat, J. *Int. J. Biol. Macromol.* **2002**, *30*, 243–249.
(31) Baugher, J. F.; Grossweiner, L. I.; Lewis, C. *J. Chem. Soc., Faraday Trans. 2* **1974**, *70*, 1389–1398.
(32) Eftink, M. R.; Ghiron, C. A. *Biochemistry* **1976**, *15*, 672–680.
(33) Lehres, S. *Biochemistry* **1971**, *10*, 3254–3263.
(34) Li, Y.; He, W.; Liu, J.; Sheng, F.; Hu, Z.; Chen, X. *Biochem. Biophys. Acta* **2005**, *1722*, 15–21.
(35) Tian, J.; Liu, J.; Hu, Z.; Chen, X. *Bioorg. Med. Acta* **2005**, *13*, 4124–4129.
(36) Lakowicz, J. R. *Principles of Fluorescence Spectroscopy*, 3rd ed.; Springer: New York, 2006.
(37) Wang, Y. Q.; Zhang, H. M.; Zhang, G. C.; Liu, S. X.; Zhou, Q. H.; Fei, Z. H. *Int. J. Biol. Macromol.* **2007**, *41*, 243–250.
(38) Bi, S. Y.; Song, D. Q.; Ding, L.; Tian, Y.; Zhou., X.; Liu, X. *Spectrochim. Acta, Part A* **2005**, *61*, 629–636.
(39) Ross, D. P.; Subramanian, S. *Biochemistry* **1981**, *20*, 3096–3099.
(40) Anand, U.; Jash, C.; Mukherjee, S. *J. Phys. Chem. B* **2010**, *114*, 15839–15845.
(41) Wang, P.; Anderko, A. *Fluid Phase Equilib.* **2001**, *186*, 103–122.